Aerodynamic Matrix Procedure for Low Aspect Ratio Wings

GEORGE W. MARTIN SR.*
Martin Company, Orlando, Fla.

A matrix method is presented for calculating the rigid and induced airload distribution for low aspect ratio wings with supersonic leading and trailing edges and inwardly raked tips. This method is applied to the static aeroelastic analysis of a set of missile fins for which experimental data is available for both the rigid and flexible cases. Comparisons are given between the theoretical and experimental values for several aerodynamic coefficients. Good agreement is shown in all cases for which data is available. The general construction of the matrices used in the aeroelastic analysis is also presented.

Nomenclature

a_{ij} = pressure coefficient induced at point j due to a unit α of aero block i
$b/2$ = wing semispan
b_{kj} = pressure coefficient induced at point j due to a unit δ of aeroblock k
C_l = rolling moment coefficient
C_p = pressure coefficient
C_N = normal force coefficient
$f(x_F, y_F)$ = $[(x - x_F)^2 - \beta^2(y - y_F)^2]^{1/2}$
$f(x_p, y_p)$ = $[(x - x_p)^2 - \beta^2(y - y_p)^2]^{1/2}$
$K_1 - K_4$ = constants used to define aerodynamic α and δ distribution
K_5, K_6 = constants used to normalize C_N and C_l data
K_7 = constant used to normalize roll rate data
L_i = load applied to structural point $i \backsim$ lb
M = Mach number
m_i = $\beta \tan \epsilon_i$
P_l, P_u = pressure on the lower and upper surface, respectively, $\backsim$ psi
q = dynamic pressure $\backsim$ psi
S = region of integration for the potential function
V = freestream velocity $\backsim$ fps
w_i = deflection of load point i
x, y = field point location
x_p, y_p = pressure point location
y_a, y_b = spanwise intersections of the forward Mach traces with the wing leading edge
y_1, y_2 = lower and upper spanwise bounds of a strip or portion of a strip that affects a pressure point
β = $(M^2 - 1)^{1/2}$
ϵ_1 = wing leading edge semi-apex angle
ϵ_2 = wing tip inward rake angle
$\alpha(B)$ = body angle of attack $\sim$ rad
$\alpha(y)$ = angle of attack distribution $\backsim$ rad
α, δ = angle of attack or incremental angle of attack, respectively, of an aerodynamic block

Introduction

IN the static aeroelastic analysis of low aspect ratio wings the effects of chordwise bending must be accounted for in both the structural and aerodynamic programs.

The change in airload distribution due to flexibility can be solved for, assuming linear aerodynamic and structural characteristics, by the methods of matrix algebra. Applying the methods of matrix theory in the same manner as in Ref. 1 to the problem of a simple wing with no control surfaces, the equilibrium deflections, under a given rigid air loading, can be obtained as follows:

$$\begin{Bmatrix} L_1 \\ \vdots \\ L_n \end{Bmatrix}_{\text{rigid}} + \begin{Bmatrix} L_1 \\ \vdots \\ L_n \end{Bmatrix}_{\text{induced}} = \begin{Bmatrix} L_1 \\ \vdots \\ L_n \end{Bmatrix}_{\text{equil}} \tag{1}$$

$$\left.\begin{aligned} \begin{Bmatrix} L_1 \\ \vdots \\ L_n \end{Bmatrix}_{\text{induced}} &= q[B][\text{corr}][A][\text{int}] \begin{Bmatrix} w_1 \\ \vdots \\ w_n \end{Bmatrix}_{\text{equil}} \\ [F] \begin{Bmatrix} L_1 \\ \vdots \\ L_n \end{Bmatrix}_{\text{equil}} &= \begin{Bmatrix} w_1 \\ \vdots \\ w_n \end{Bmatrix}_{\text{equil}} \end{aligned}\right\} \tag{2}$$

or

$$\begin{Bmatrix} L_1 \\ \vdots \\ L_n \end{Bmatrix}_{\text{equil}} = [F]^{-1} \begin{Bmatrix} w_1 \\ \vdots \\ w_n \end{Bmatrix}_{\text{equil}} = [S] \begin{Bmatrix} w_1 \\ \vdots \\ w_n \end{Bmatrix}_{\text{equil}} \tag{3}$$

combining (1, 2, and 3)

$$\begin{Bmatrix} L_1 \\ \vdots \\ L_n \end{Bmatrix}_{\text{rigid}} + q[B][\text{corr}][A][\text{int}] \begin{Bmatrix} w_1 \\ \vdots \\ w_n \end{Bmatrix}_{\text{equil}} = [S] \begin{Bmatrix} w_1 \\ \vdots \\ w_n \end{Bmatrix}_{\text{equil}} \tag{4}$$

which reduces to

$$[[S] - q[B][\text{corr}][A][\text{int}]]^{-1} \begin{Bmatrix} L_1 \\ \vdots \\ L_n \end{Bmatrix}_{\text{rigid}} = \begin{Bmatrix} w_1 \\ \vdots \\ w_n \end{Bmatrix}_{\text{equil}} \tag{5}$$

where

$[S]$ = stiffness matrix in which the coefficients relate the loads at the structural load points to the deflections of these points $\sim$ lb/in.
$[F]$ = flexibility matrix in which the coefficients relate the deflection of the structural load points to the applied loads at these points $\sim$ in./lb.
q = dynamic pressure, psi
$[B]$ = matrix used to apply the airloads to the structural load points $\sim$ in.
[corr] = empirical matrix used to correct the predicted aerodynamic load distribution when the appropriate test data is available.
$[A]$ = aerodynamic matrix in which the coefficients relate the loading, per unit q, over the wing to the unit α or δ of a prescribed segment of the wing.
[int] = interpolation matrix used to convert from the structural deflections defined by the structural matrix to the α and δ distribution required for the aerodynamic matrix.

Received December 31, 1963; revision received May 4, 1964. The author wishes to thank S. Cook for the use of the test data presented in this paper. He also thanks V. L. Hining for his supervision of the structural influence coefficient test and C. Casteleiro and G. Logan for supplying the experimental aerodynamic data presented.

* Aerodynamics Section Head, Air Loads Analysis.

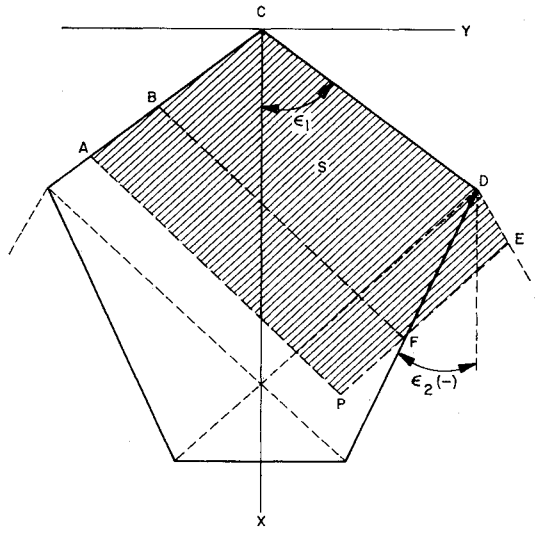

Fig. 1 Area of integration for ϕ in the tip region.

$\begin{Bmatrix} L_1 \\ \vdots \\ L_n \end{Bmatrix}_{\text{equil}}$ = column matrix of equilibrium loads applied to the structural load points.

$\begin{Bmatrix} L_1 \\ \vdots \\ L_n \end{Bmatrix}_{\text{rigid}}$ = column matrix of rigid loads applied to the structural load points

$\begin{Bmatrix} L_1 \\ \vdots \\ L_n \end{Bmatrix}_{\text{induced}}$ = column matrix of induced loads applied to the structural load points

$\begin{Bmatrix} w_1 \\ \vdots \\ w_n \end{Bmatrix}_{\text{equil}}$ = due to the applied rigid load

The change in airloads due to flexibility can be obtained from (2) using the results of (5), and the final airload distribution is then obtained from (1).

The total load or moments due to the distributed loading can be obtained by using an integrating matrix $[I]$:

$$[I]\begin{Bmatrix} L_1 \\ \vdots \\ L_n \end{Bmatrix}_{\text{equil}} = \begin{Bmatrix} \text{load} \\ \text{pitching moment} \\ \text{rolling moment} \end{Bmatrix} \tag{6}$$

The required structural matrix is obtained by either analytical or experimental means and all other matrices, with the exception of the aerodynamic matrix, can be obtained from the geometry of the wing and the location of the structural load points.

The required aerodynamic matrix is the major topic of this paper. The method presented here is an extension of Ref. 2 and is applicable to wings with supersonic leading and trailing edges and inwardly raked tips. The effect of interacting tip regions required for low aspect ratio wings is included. A sample wing is shown for which experimental data is available for both the rigid and flexible cases. Comparisons are given between the predicted and experimental values obtained in both cases.

Aerodynamic Matrix Procedure

The lifting pressure distribution on a thin wing, moving at supersonic speed, can be obtained by replacing the wing with a zero thickness plate in the shape of the camber surface of the original wing. A potential function ϕ is available from which the pressure distribution can be obtained. The potential equation, as presented in Ref. 3, is

$$\phi = -\frac{V}{\pi}\iint_S \frac{\alpha(x, y)dydx}{[(x - x_p)^2 - \beta^2(y - y_p)^2]^{1/2}} \tag{7}$$

where S is the region of integration as defined by the forward Mach traces and the planform geometry.

The total lifting pressure coefficient C_p can be obtained from Eq. (7) since it is directly related to the potential:

$$C_p = \frac{P_l - P_u}{q} = -\frac{4}{V}\frac{\partial\phi}{\partial x} = \frac{4}{\pi}\frac{\partial}{\partial x}\iint_S \frac{\alpha(x, y)dydx}{[(x - x_p)^2 - \beta^2(y - y_p)^2]^{1/2}} \tag{8}$$

In the regions of the wing in which S is contained within the boundaries of the wing only, the pressure coefficient can be obtained from Eq. (8) as follows:

$$C_p = \frac{4}{\pi}\left\{\iint_S \frac{\partial\alpha/\partial x dydx}{[(x - x_p)^2 - \beta^2(y - y_p)^2]^{1/2}} + \int_{y_a}^{y_b} \frac{\alpha dy}{[(x - x_p)^2 - \beta^2(y - y_p)^2]^{1/2}}\right\} \tag{9}$$

where y_a and y_b are the spanwise limits of the intersections of the forward Mach traces with the wing leading edge with the line integral taken along the wing leading edge.

In the tip regions, the area S includes both regions of the wing and the upwash field associated with the tip regions. The upwash field, influencing the pressure distribution in this tip region, is shown in Fig. 1.

The area cancellation procedure presented by Evvard[4] can be utilized to eliminate the upwash calculation in the region DEF of Fig. 1. The area cancellation is used in the evaluation of $\partial\phi/\partial x$, using the boundary condition that $C_p = 0$ along the subsonic trailing edge of the raked tip rather than $\phi = 0$ as is used on a streamwise tip or subsonic leading edge:

$$C_{p_{x_p,y_p}} = \frac{4}{\pi}\left\{\int_A^B \frac{\alpha dy}{f(x_p, y_p)} + \iint_{ABFP} \frac{\partial\alpha/\partial x dydx}{f(x_p, y_p)}\right\} + \frac{4}{\pi}\left\{\int_B^C \frac{\alpha dy}{f(x_p, y_p)} + \int_C^D \frac{\alpha dy}{f(x_p, y_p)} - \int_F^D \frac{\alpha dy}{f(x_p, y_p)} + \iint_{BCDF} \frac{\partial\alpha/\partial x dydx}{f(x_p, y_p)} + \iint_{DEF} \frac{\partial\alpha/\partial x dydx}{f(x_p, y_p)} + \int_D^E \frac{\alpha dy}{f(x_p, y_p)}\right\} \tag{10}$$

$$C_{p_{x_F,y_F}} = 0 = \frac{4}{\pi}\left\{\int_B^C \frac{\alpha dy}{f(x_F, y_F)} + \int_C^D \frac{\alpha dy}{f(x_F, y_F)} - \int_F^D \frac{\alpha dy}{f(x_F, y_F)} + \iint_{BCDF} \frac{\partial\alpha/\partial x dydx}{f(x_F, y_F)} + \iint_{DEF} \frac{\partial\alpha/\partial x dydx}{f(x_F, y_F)} + \int_D^E \frac{\alpha dy}{f(x_F, y_F)}\right\} \tag{11}$$

Evvard has shown that Eq. (11) can be used to eliminate the corresponding line and surface integrals in Eq. (10). The

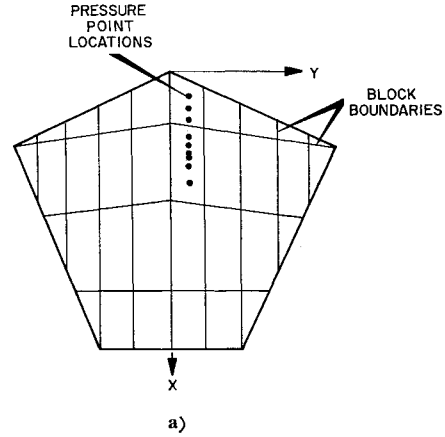

a)

Fig. 2 Block division and point locations.

pressure coefficient evaluated at x_p, y_p therefore reduces to

$$C_{p_{x_p,y_p}} = \frac{4}{\pi}\int_A^B \frac{\alpha dy}{[(x-x_p)^2-\beta^2(y-y_p)^2]^{1/2}} + \frac{4}{\pi}\iint_{ABFP} \frac{\partial\alpha/\partial x dy dx}{[(x-x_p)^2-\beta^2(y-y_p)^2]^{1/2}} \quad (12)$$

In the matrix technique used subsequently, it is assumed that $\alpha = \alpha(y)$ for a given wing which eliminates the surface integral and allows C_p to be defined only by the line integral

$$C_{p_{x_p,y_p}} = \frac{4}{\pi}\int_A^B \frac{\alpha dy}{[(x-x_p)^2-\beta^2(y-y_p)^2]^{1/2}} \quad (13a)$$

By a similar technique, the pressure coefficient in the region affected by both tips can be evaluated.

Case I. Reflected traces do not cross on the planform:

$$C_p = \frac{4}{\pi}\int_A^B \times \frac{\alpha dy}{[(x-x_p)^2-\beta^2(y-y_p)^2]^{1/2}} \quad (13b)$$

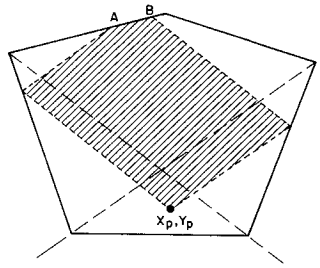

Case II. Reflected traces cross on the planform:

$$C_p = -\frac{4}{\pi}\int_A^B \times \frac{\alpha dy}{[(x-x_p)^2-\beta^2(y-y_p)^2]^{1/2}} \quad (13c)$$

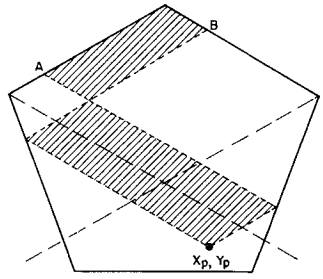

It is important to note that the line integrals along the reflected traces used for points in the influence of a subsonic leading edge are not encountered here. These line integrals are eliminated because of the change in boundary condition from $\phi = 0$ at the leading edge for a subsonic leading edge wing to $\partial\phi/\partial x = 0$ along the raked tip used in this analysis.

Superposition Technique

Because of the linearity of the basic potential function ϕ a matrix can be constructed relating linearly the pressure induced at a point on the wing to the unit rotation, α or δ, of a given segment of the wing.

The coefficients of the aerodynamic matrix are constructed as follows: 1) the wing planform is divided into a series of blocks over which α is assumed to be constant, and 2) a series of pressure point locations is distributed over the wing surface in any manner desired (see Fig. 2). The pressure induced at a point x_p, y_p can then be found from the following relation:

$$C_{p_j} = \sum_{i=1}^{N} a_{ij}\alpha_i \quad (14)$$

where N is the total number of wing block divisions, a_{ij} the pressure coefficient induced at point j due to a unit α of block i, and α_i the angle of attack of block i.

Equation (14) can be transposed to a more easily handled form as follows:

$$C_{p_j} = \sum_{i=1}^{J} a_{ij}\alpha_i + \sum_{K=1}^{(N-J)} b_{kj}\delta_k \quad (15)$$

where J is the total number of blocks i along the wing leading edge; a_{ij} and α_i are as previously defined; b_{kj} is the pressure coefficient induced at point j due to a unit rotation of the region contained between the leading edge of block K, the wing trailing edge, and the spanwise boundaries of block K; and δ_k is the difference between the angle of attack of block K and the region immediately upstream of block K.

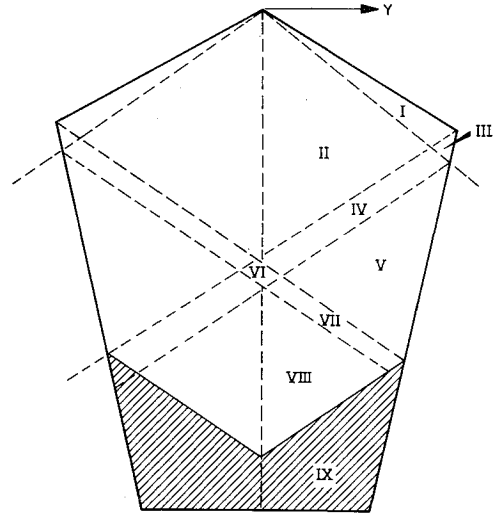

Fig. 3 Nine pressure point regions.

In using Eqs. (13) to evaluate the terms of the pressure coefficient matrix the superposition technique used in Ref. 2 is employed. The locations of the pressure points and all the equations presented are again referenced to the location of the apex of the wing or subwing being analyzed.

Intersection Equations for Camber Matrix

The method for calculating the pressure distribution covers the nine regions of Fig. 3. In all cases it is assumed that $\partial\alpha/\partial x = 0$ so that the only term affecting the pressure at a point is of the form

$$\frac{4}{\pi}\int_{y_a}^{y_b} \frac{\alpha dy}{[(x-x_p)^2-\beta^2(y-y_p)^2]^{1/2}} \quad (16)$$

The pressure coefficient equation for all cases in regions I–VI then will be of the same basic form. The C_p induced at a point in regions VII or VIII, when the forward Mach traces cross on the planform, is of the form

$$-\frac{4}{\pi}\int_{y_a}^{y_b} \frac{\alpha dy}{[(x-x_p)^2-\beta^2(y-y_p)^2]^{1/2}} \quad (17)$$

The solutions of Eq. (16) for strips or portions of strips that lie within the bounds $y_a \leq y \leq y_b$ as given in Ref. 2 are 1) strips on the left side of the wing,

$$C_{p_{(x_p,y_p)}} = \frac{4m_1\alpha}{\beta\pi(m_1^2-1)^{1/2}} \times \left[\sin^{-1}\frac{(m_1^2-1)(\beta y_2/m_1) - x_p - m_1\beta y_p}{\beta y_p + m_1 x_p} - \sin^{-1}\frac{(m_1^2-1)(\beta y_1/m_1) - x_p - m_1\beta y_p}{\beta y_p + m_1 x_p}\right] \quad (18)$$

and 2) strips on the right side of the wing,

$$C_{p_{(x_p,y_p)}} = \frac{4m_1\alpha}{\beta\pi(m_1^2-1)^{1/2}} \times \left[\sin^{-1}\frac{(1-m_1^2)(\beta y_2/m_1) - x_p + m_1\beta y_p}{\beta y_p - m_1 x_p} - \sin^{-1}\frac{(1-m_1^2)(\beta y_1/m_1) - x_p + m_1\beta y_p}{\beta y_p - m_1 x_p}\right] \quad (19)$$

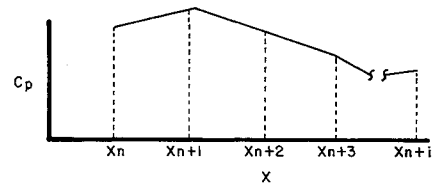

Fig. 4 Linear integration intervals.

where

$\beta = (M^2 - 1)^{1/2}$
ϵ_1 = wing semiapex angle
$m_1 = \beta \tan\epsilon_1$
y_1, y_2 = lower and upper spanwise bounds of a strip or portion of a strip that affects a point

The solutions for Eq. (17) are identical with (18) and (19) except for a change in sign.

The required limits of integration, used in programing this procedure, for a pressure point in any of the nine regions are given in Tables 1 and 2.

Special Equations

$$x_{R_1} = \frac{1}{1+m_2}\left[\beta\frac{b}{2}\left(\frac{m_2}{m_1}-1\right)+\beta y_p + x_p\right]$$

$$y_{R_1} = \frac{b}{2} + \frac{m_2}{\beta}\left[x_{R_1} - \frac{\beta}{m_1}\frac{b}{2}\right]$$

$$x_A = \frac{\beta b/2}{m_2 - 1}\left[\frac{m_2}{m_1} - \frac{1}{m_1} - 2\right]$$

$$y_A = \frac{x_A}{\beta} - \frac{b}{2}\left[\frac{1}{m_1} + 1\right]$$

where

$m_2 = \pi\tan\epsilon_2$
ϵ_2 = inward rake angle of the tip

$$x_{L_1} = \frac{\beta}{1+m_2}\left[\frac{b}{2}\left(\frac{m_2}{m_1}-1\right) - y_p + \frac{x_p}{\beta}\right]$$

$$y_{L_1} = -\frac{b}{2} - \frac{m_2}{\beta}\left[x_{L_1} - \frac{\beta}{m_1}\frac{b}{2}\right]$$

$$x_{\text{int}} = \tfrac{1}{2}[x_{L_1} + x_{R_1} + \beta(y_{L_1} - y_{R_1})]$$

$$y_{\text{int}} = y_{R_1} + \frac{1}{\beta}(x_{\text{int}} - x_{R_1})$$

Special Condition, Region IX

If $X_p > X_A + \beta Y_A - \beta Y_p$, set $C_p = 0$ for all strips. This sets the limitation on the number of reflections that can be accounted for. In this case all points that fall behind the reflected tip trace of the wing being analyzed, are assumed unaffected by the wing. Special coding instructions are needed for the case of an unswept wing since $\tan\epsilon \to \infty$ as $\epsilon \to 90°$. These instructions are given in the same order as

Special Equations

$$x_{R_2} = \frac{1}{1+m_2}\left(\beta y_p + x_p - \beta\frac{b}{2}\right)$$

$$y_{R_2} = \frac{b}{2} + \frac{m_2}{\beta}x_{R_2}$$

$$x_B' = 2\left[\frac{\beta(b/2)}{1-m_2}\right] \qquad y_B' = \frac{b}{2}\left[\frac{2}{1-m_2} - 1\right]$$

$$x_{L_2} = \frac{\beta}{1+m_2}\left[-\frac{b}{2} - y_p + \frac{x_p}{\beta}\right]$$

$$y_{L_2} = -\frac{b}{2} - \frac{m_2}{\beta}x_{L_2}$$

$$x_{\text{int}}' = \tfrac{1}{2}[x_{L_2} + x_{R_2} + \beta(y_{L_2} - y_{R_2})]$$

If $X_p > (X_B' + \beta Y_B' - \beta Y_p)$ set $C_p = 0$ for all strips of the wing being analyzed. The C_p equation used for all strips or parts of strips for an unswept wing is

$$C_p = \frac{4\alpha}{\beta\pi}\left[\sin^{-1}\frac{\beta(y_2 - y_p)}{x_p} - \sin^{-1}\frac{\beta(y_1 - y_p)}{x_p}\right] \quad (20)$$

A change of sign is again used when the forward Mach traces cross on the planform.

Table 1 Limits of integration, swept leading edge

Regions	Boundary condition	Limits of integration: Left side	Limits of integration: Right side
I and II	$x_p \le \beta\frac{b}{2}\left(\frac{m_1+1}{m_1}\right) - \beta y_p$	$\frac{m_1}{\beta}\frac{(\beta y_p - x_p)}{(m_1+1)} \le y \le 0$	$\frac{m_1}{\beta}\frac{(\beta y_p - x_p)}{(m_1-1)} \le y \le \frac{m_1}{\beta}\frac{(x_p + \beta y_p)}{(m_1+1)}$
III–V	$\beta\frac{b}{2}\left(\frac{m_1+1}{m_1}\right) - \beta y_p < x_p \le \beta\left[y_p + \left(\frac{m_1+1}{m_1}\right)\frac{b}{2}\right]$	$\frac{m_1}{\beta}\frac{(\beta y_p - x_p)}{(m_1+1)} \le y \le \frac{m_1}{\beta}\frac{(\beta y_{R_1} - x_{R_1})}{(1+m_1)}$	$\frac{m_1}{\beta}\frac{(\beta y_p - x_p)}{(m_1-1)} \le y \le \frac{m_1}{\beta}\frac{(x_{R_1} - \beta y_{R_1})}{(1-m_1)}$
VI–VIII	$x_A + \beta y_A - \beta y_p \ge x_p > \beta\left[y_p + \left(\frac{m_1+1}{m_1}\right)\frac{b}{2}\right]$	...	...
	a) $m_1 x_{\text{int}} \le -\beta y_{\text{int}}$	$\frac{m_1}{\beta(m_1-1)}(\beta y_{L_1} + x_{L_1}) \le y \le \frac{m_1}{\beta(m_1+1)}(\beta y_{R_1} - x_{R_1})$	$\frac{m_1}{\beta(m_1+1)}(\beta y_{L_1} + x_{L_1}) \le y \le \frac{m_1}{\beta(1-m_1)}(x_{R_1} - \beta y_{R_1})$
	(reflected traces do not cross on the planform)		
	b) $m_1 x_{\text{int}} > -\beta y_{\text{int}}$	$\frac{m_1}{\beta(1+m_1)}(\beta y_{R_1} - x_{R_1}) \le y \le \frac{m_1}{\beta(m_1-1)}(\beta y_{L_1} + x_{L_1})$	$\frac{m_1}{\beta(1-m_1)}(x_{R_1} - \beta y_{R_1}) \le y \le \frac{m_1}{\beta(m_1+1)}(\beta y_{L_1} + x_{L_1})$
	(reflected traces cross on the planform)		

Integration Procedure

The preceding section presents the method used to compute a matrix of aerodynamic influence coefficients relating the pressure induced at a point to the unit α or δ of a fixed region of the wing. An aerodynamic matrix can in turn be constructed which relates the $c_l c$ induced over a given incremental x length, with y fixed, to the unit α or δ of the fixed region of the wing. This is accomplished by integrating the calculated pressure coefficient distribution.

The pressure coefficient matrix $[A_{cp}]$ is in the form

$$[A_{cp}] = \begin{bmatrix} a_{11} & a_{12} & \cdots & a_{in} \\ \cdot & & & \cdot \\ \cdot & & & \cdot \\ \cdot & & & \cdot \\ \cdot & & & \cdot \\ a_{m_1} & a_{m_2} & \cdots & a_{mn} \end{bmatrix}$$

where aij relates the pressure coefficients induced at point i due to a unit α or δ of wing segment j.

The integrated matrix is of the same general form with the exception that the coefficients relate the value of

$$\int_{x_n}^{x_{n+i}} C_p dx$$

obtained because of the unit α or δ of the prescribed wing segment. This is shown graphically in Fig. 4. The equations used to integrate the given equations are obtained by linear interpolation between points.

$$\int_{x_n}^{x_{n+i}} C_p dx = \sum_{N=n}^{N=(n+i-1)} (C_{p_{x_{N+1}}} + C_{p_{x_N}}) \frac{(x_{N+1} - x_N)}{2} \quad (21)$$

If a pitching moment matrix is required, the integration takes the form

$$\int_{x_n}^{x_{n+i}} C_p x dx = \sum_{N=n}^{N=(n+i-1)} \left\{ C_{p_{x_N}} (x_{N+1} - x_N) \times \left(\frac{x_{N+1} + x_N}{2} \right) - (C_{p_{x_N}} - C_{p_{x_{N+1}}}) \times \left(\frac{x_{N+1} - x_N}{2} \right) [x_N + \tfrac{2}{3}(x_{N+1} - x_N)] \right\} \quad (22)$$

The terms of the moments matrix would then relate the incremental value of

$$\int_{x_n}^{x_{n+i}} C_p x dx$$

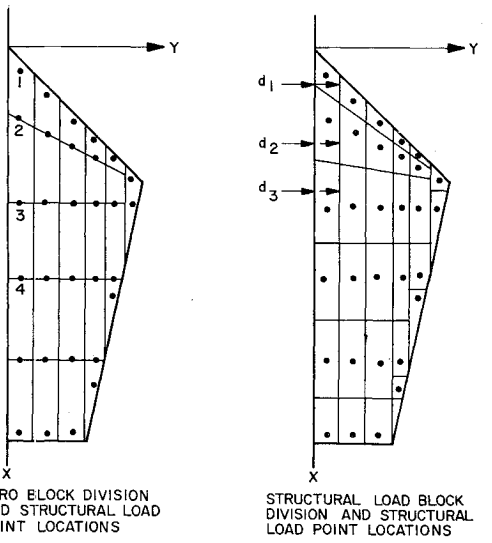

Fig. 5 Aero block, structural block, and structural load point locations.

obtained over the desired segments of the given chord because of a unit α or δ of a fixed segment of the wing.

Construction of the Aeroelasticity Matrices

The aerodynamic method presented was used to predict the aeroelastic effect on the air load distributions of the wing shown in Fig. (5). The load conditions analyzed were for the following:

1) Wing at angle of attack: $(\alpha_B = 0)$, $\alpha(y) = K_1$
2) Wing at angle of attack with the aerodynamic wing α distribution determined from Beskins' upwash equation of Ref. 5: $\alpha(y) = \alpha_B\{1 + [R_B^2/(R_B + y)^2]\}$
3) Rolling configuration: $(\alpha_B = 0)$, $\alpha(y) = K_2 + K_3 y$
4) Rolling moment due to a bend tab at the wing trailing edge: $\delta = K_4$

In the aeroelastic analysis of the four preceding load conditions it was assumed that the body acted as a complete reflection surface. The effect of the flexibility on the rolling moment produced by a single wing panel was then investigated in each of the load conditions.

The general construction of the matrices required in the aeroelastic loop is presented in this section. The required

Table 2 Limits of integration, unswept leading edge

Regions	Boundary condition	Limits of integration (only one equation required for both sides)
I and II	$x_p \leq \beta\left(\frac{b}{2} - y_p\right)$	$y_p - \frac{x_p}{\beta} \leq y \leq y_p + \frac{x_p}{\beta}$
III–V	$\beta\left(\frac{b}{2} - y_p\right) < x_p \leq \beta\left(y_p + \frac{b}{2}\right)$	$y_p - \frac{x_p}{\beta} \leq y \leq \frac{1}{\beta}(\beta y_{R_2} - x_{R_2})$
VI–VIII	$x_B' + \beta y_B' - \beta y_p \leq x_p < \beta\left(y_p + \frac{b}{2}\right)$	...
	a) $x_{\text{int}}' \leq 0$ reflected traces do not cross on the planform	$\frac{1}{\beta}(\beta y_{L_2} + x_{L_2}) \leq y \leq \frac{1}{\beta}(\beta y_{R_2} - x_{R_2})$
	b) $x_{\text{int}}' > 0$ (reflected traces cross on the planform)	$\frac{1}{\beta}(\beta y_{R_2} - x_{R_2}) \leq y \leq \frac{1}{\beta}(\beta y_{L_2} + x_{L_2})$

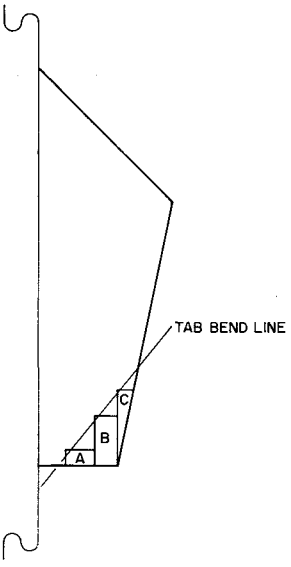

Fig. 6 Aero block division used to represent the bent tab.

structural flexibility matrix was determined experimentally under the supervision of V. L. Hining of the Martin Company.

The $[B]$ matrix was constructed assuming that the loading calculated at the centerline of the structural load block represented the average loading over the block. The load on a block, which is applied to the corresponding load point, then is the local loading along the centerline times the width of the block.

$$[B] = \begin{bmatrix} d_1 & & & & \\ & d_2 & & & \\ & & d_3 & & \\ & & & \ddots & \\ & & & & d_n \end{bmatrix}$$

The wing division for the aerodynamic matrix, the structural load block division, and the structural load points are shown in Fig. 5.

The chordwise and spanwise bounds for the structural load block division were obtained by bisecting the chordwise dimension between points and spanwise dimension between rows of points, respectively. All the load calculated in any structural load block division was then beamed to the structural load point contained in that block.

The α for the aerodynamic blocks is taken as the difference in deflection between the front and rear load points divided by the distance between them, i.e.,

$$\alpha_1 = (w_2 - w_1)/(x_2 - x_1) \qquad (23)$$

Since the required aerodynamic distribution is in the form of

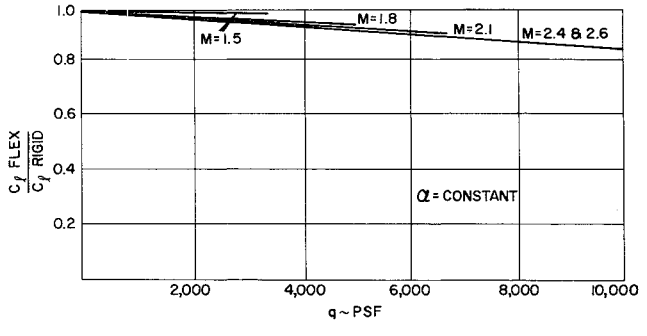

Fig. 7 Typical curve for the flexibility effects on load conditions 1, 2, and 3.

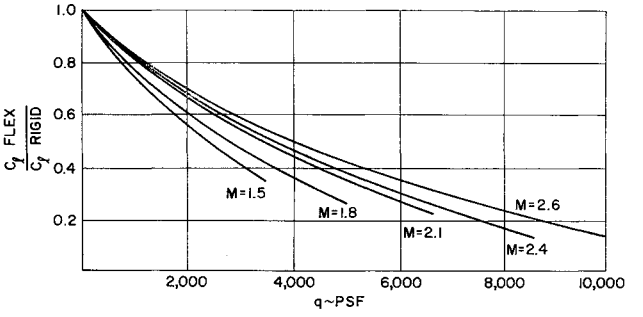

Fig. 8 Flexibility effects on load condition 4.

α and δ, the required interpolation matrix is obtained by subtracting the appropriate α's defined by Eq. (23) to obtain the required δ's. (Note that, as explained before, the leading edge blocks are the only ones that use the α distribution.) The correlation matrix was a unit diagonal matrix since pure theory was used throughout the analysis.

The integrating matrix (I) is of the form

$$[I] = \begin{bmatrix} 1 & 1 & 1 & 1 & \cdots & 1 \\ x_1 & x_2 & x_3 & x_4 & \cdots & x_n \\ y_1 & y_2 & y_3 & y_4 & \cdots & y_n \end{bmatrix}$$

where X_i and Y_i are the distances of load point i from the pitch and roll axes, respectively.

The required rigid loads are calculated simply by the matrix product:

$$\begin{Bmatrix} L_1 \\ \vdots \\ L_n \end{Bmatrix}_{\text{rigid}} = q[B][A] \begin{Bmatrix} \alpha_1 \\ \vdots \\ \delta_m \end{Bmatrix}_{\text{rigid}}$$

using the matrices of the aeroelastic loop. The column matrix of the rigid α and δ distribution is input for the desired loading. The δ distribution for the loading due to the bent tab was approximated by setting $\delta = K_4$ for regions A, B, and C of Fig. 6.

The aerodynamic procedure presented was used to evaluate the change in roll rate due to aeroelastic effects on the missile fin shown in Fig. 5. The roll rate was to be produced by the bent tab at the trailing edge of the fin as shown in Fig. 6.

The calculated flex/rigid ratios are shown in Figs. 7 and 8 for the load conditions. Figure 8 presents the results for load conditions 1, 2, and 3, since they were identical. Comparisons are also given in Figs. 9 and 10 between the predicted and experimental rigid values of normal force coefficient on the fin with body at angle of attack (load condition 2) and the rolling moment coefficient per degree of tab deflection for several tab bend angles (load condition 4). Good agreement is shown in both cases.

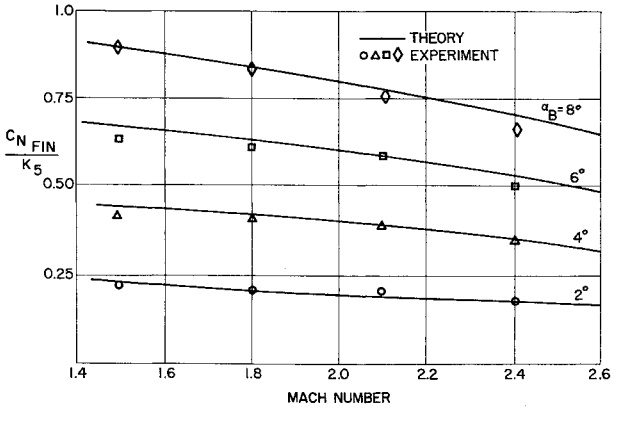

Fig. 9 Comparison of experimental and theoretical fin loads.

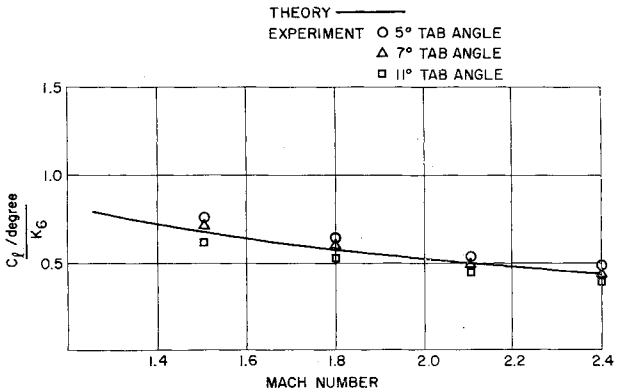

Fig. 10 Comparison of experimental and theoretical bent tab rolling effectiveness.

The normal force coefficients for fin alone were obtained from test data using the K factors of Ref. 6 as follows:

$$C_{N_{\text{fin}}} = \frac{K_{W(B)}}{K_{W(B)} + K_{B(W)}} (C_{N_{\text{body and fin}}} - C_{N_{\text{body alone}}})$$

The analytical results in Figs. 7 and 8 showed that the roll rate would vary greatly as a function of dynamic pressure and would be degraded from the desired value due to flexibility effects. The change in roll rate at a given value of q and Mach number could be obtained as follows:

$$\% \text{ change} = 100 \left(\frac{[C_{l_{\text{flex}}}/C_{l_{\text{rigid}}}]_{\text{bent tab}}}{[C_{l_{\text{flex}}}/C_{l_{\text{rigid}}}]_{\text{roll damping}}} - 1 \right) \quad (24)$$

In the initial test shots the predicted loss in roll rate was substantiated as is shown in Fig. 11.

The correction for this flexibility problem was obtained by inspecting the effect of flexibility on load condition 2, i.e., using a differential fin incidence, with $\alpha_B = 0$, as the exciting force in roll. The flex to rigid ratios in this case were very similar to that of the damping in roll case, load condition 3, which would indicate that flexibility would not affect the roll rate to any extent, referring to Eq. (24) again. Subsequent tests using the differential wing incidence as the roll producing device, again substantiated the predicted values.

Conclusions

A rapid method for calculating rigid or flexible airload distributions has been presented. (As an indication of the speed of the coded program, the runs for the data in this paper consumed approximately one minute for each Mach number on the IBM 7094. This run time includes the calculation of the aerodynamic matrix and the rigid loads for the four load conditions analyzed in addition to the static aeroelastic solution for each one of these conditions at seven values of q). Comparisons were given between experimental data and theoretical predictions for a specific configuration, using both rigid model and flexible model data, and good agreement was shown in all cases.

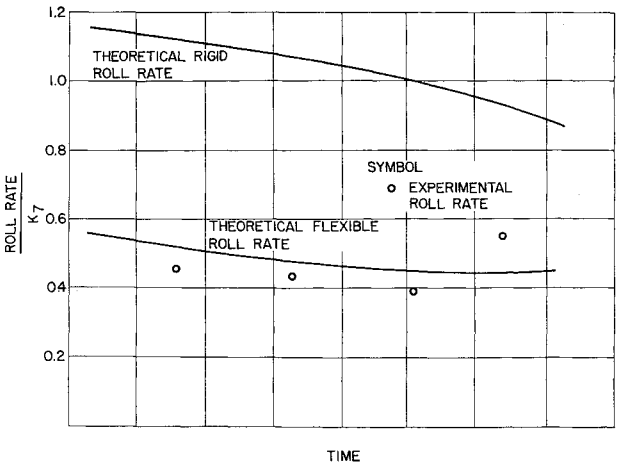

Fig. 11 Roll rate comparison.

References

[1] Johnson, W. S., "An aeroelastic procedure for flap-type control surfaces," J. Aerospace Sci. **28**, 985–987 (1961).

[2] Johnson, W. S. and Martin, G. W., "An aerodynamic-influence coefficient procedure for wings having supersonic trailing edges and streamwise tips," Aerospace Eng. **20**, 22–23, 76–80 (September 1961).

[3] Carafoli, E., *High Speed Aerodynamics (Compressible Flow)* (Pergamon Press, New York, 1956), Chap. VIII, pp. 478–481.

[4] Evvard, J. C., "Use of source distribution for evaluating theoretical aerodynamics of thin finite wings at supersonic speeds," NACA Rept. 951, pp. 1–10 (1950).

[5] Beskin, L., "Determination of upwash around a body of revolution at supersonic velocities," Rept. CM-251, John Hopkins University, Applied Physics Lab. (May 27, 1946).

[6] Pitts, W. C., Nielsen, J. N., and Kaattari, G. E., "Lift and center of pressure of wing-body-tail combinations at subsonic, transonic, and supersonic speeds," NACA Rept. 1307-5, p. 49 (1959).